Assessment of the Carbon and Cost Savings of a Combined Diesel Generator, Solar Photovoltaic, and Flywheel Energy Storage Islanded Grid System

Mustafa E. Amiryar * and **Keith R. Pullen ***

School of Mathematics, Computer Science and Engineering at City, University of London, London EC1V 0HB, UK
* Correspondence: mustafa.amiryar.2@city.ac.uk (M.E.A.); k.pullen@city.ac.uk (K.R.P.);
Tel.: +44-(0)20-7040-3475 (K.R.P.)

check for updates

Abstract: The use of diesel generators to provide power for islanded grids has been the technology of choice but they generate substantial carbon emissions unless the part or all the fuel comes from a renewable source. Notwithstanding this, the engine must be sized to meet maximum demand and will operate inefficiently at part load most of the time, which is particularly bad for a synchronous constant speed engine. Given the availability of low cost solar photovoltaic (PV) systems, it is very enticing to fit a diesel generator and allow the engine to be turned off during PV generation. However, this combination will not work without some form of energy storage since it takes time for the engine to start, leading to gaps in supply and instability of the system. Lithium-ion batteries are typically considered to be the best solution to this problem because they have a high response rate, costs are lower, and they are available as products. However, they will suffer from the limited cycle and calendar life due to high cycling requirements in the application described. It is, therefore, proposed that a flywheel system could offer a lower lifetime cost alternative since only short duration bridging power storage is needed and flywheels of appropriate design can offer lower power cost than Lithium-ion battery systems. Flywheels are particularly attractive since they have a very high calendar with almost an infinite cycle life and are fully recyclable at the end of life. This research, therefore, presents an assessment of the flywheel energy storage system (FESS) as an alternative to electrochemical batteries to supplement solar PV systems backed up by diesel generators. The model of an islanded PV system combined with a diesel generator and a FESS supplying power to a residential load is implemented in MATLAB/Simulink. The results of the analysis for the cases with and without storage based on a number of different charge-discharge strategies provide evidence to support this hypothesis.

Keywords: flywheel energy storage; solar photovoltaic system; backup diesel generator; dynamic model; standalone hybrid system

1. Introduction

Renewable energy sources (RES), typically in the form of distributed generation (DG), can be considered supplements or even substitutes to traditional generation [1,2]. It is vital to meet the growing global energy demand by as much RES as possible in order to mitigate climate change. RES largely contributes toward facilitating clean and emission-free energy and increasing the energy supply while decreasing carbon footprints. However, the major challenge associated with the energy demand coming from the renewables is their intermittent nature across a range of timescales that will lead to reliability problems [3,4]. In addition, the traditional approach of controlling the energy generation and load demand during peak times by installing gas turbine generators will no longer be an ideal solution given their environmental impacts.

The solution to the problem of balancing can be met by using energy storage systems (ESS), which are now a necessity to combine with traditional generating plants to meet an excess demand and balance the intermittent RES integrated to electrical networks [5]. They are needed at different points within an electricity grid from generation to the customer level to supplement electrical energy generation and demand [1,6]. At the distribution level, energy storage is typically needed to complement DGs providing back up for uninterruptible power supply (UPS) services. DGs are mostly located at the customer level in order for the power to be generated at the scales demanded by the consumers and at the point where it is being consumed. However, for smaller capacity of generation (kW to a few MW) and a higher possibility of line faults in DGs create load variations and voltage drops, which further lead to stability problems at the distribution level. Integration of storage systems with DGs provide power flexibility and improve system stability. Penetration of DG will be more robust and further supported by advancements in energy storage technologies as well as availability of RES [5].

It is, therefore, important to keep the AC supply frequency within a certain range to avoid a system collapse. The stability issue at the distribution level has been generally addressed with a combination of demand-side management and energy storage, where the former can alternatively be used as a balancing mechanism to manage the unbalancing issue of demand and generation by postponing the power draw from the equipment with the slower time constant. However, this is already being implemented and other ways must be sought to time-shift the demand. The energy storage part is mainly dominated by the use of large banks of Li-ion batteries where they can encounter the sub-second response with suitable control electronics capable of providing typical durations of one to two hours. This will allow added revenue streams such as arbitrage, load-shifting, and other grid ancillary services including long-duration energy storage services, as shown in Figure 1. Hence, more attention was drawn toward Li-ion batteries and low storage, but high-power technologies such as supercapacitors and flywheels have been disadvantaged to compete with them. The question might be whether other technologies can be considered to replace the deployment of large numbers of grid-scale Li-ion batteries to meet growing future storage needs? The answer to this question is not simple because there are other factors that will affect the future of storage with a number of interdependencies [7].
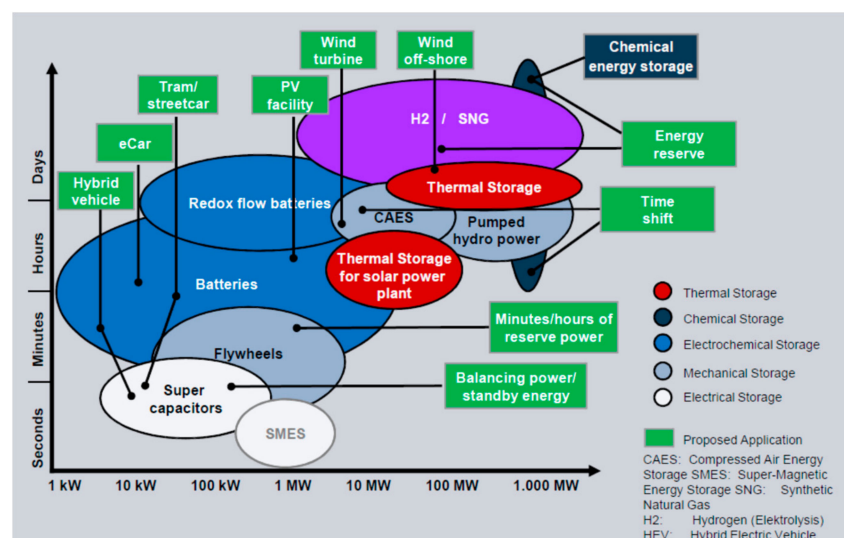
Figure 1. Energy storage technologies concerning typical charge-discharge timescales and available power [8].

The lack of recycling of Li-ion batteries and their production relying on materials from questionable sources is already a concern [9]. On the technical part, high penetration of renewables and DG as well

as potential deployment of electric vehicles will significantly affect the balance of the electrical grid. The balancing problem could be mitigated with the integration of a good fit storage system as well as by delaying the charging periods of the electric vehicles to periods of low demand. However, this is limited by the nature and characteristics of a Li-ion battery, where its lifetime will be compromised due to multiple charging or deep discharging, as addressed in detail in reference [10].

Lastly, the structure of the energy market is in the reformation process from a traditional system of large centralized units with peaking plants to one fit for purpose for a system with high dispersion of RES, DGs, and prosumers [7]. This demands energy storage technologies should respond accordingly. In the past, ESS were mainly rated based on their energy capacity (in GWh) with one cycle per day. However, today, the same systems could be used up to 10 and 20 times a day, making the power capacity more important than the energy capacity [4].

There is a necessity to further reduce the cost of energy storage by employing easily recyclable technologies with lower CO_2 emissions and lifetimes of more than 20 years, unlike Li-ion batteries. Flow batteries, compressed or liquid air, pumped hydro, gravity systems, and engines operating based on renewable fuels can be better candidates. Nevertheless, the sub-second response from the start-up cannot be met by any of the mentioned technologies, which leaves a gap to be filled. If Li-ion batteries are used to meet this gap, in addition to their main issue of suffering from a limited cycle life, an overlap of the provision in storage duration will also be an issue. Therefore, the optimal choice will be technology with low minutes of storage and lowest cost and the flywheel storage fits this perfectly.

To make more use of ESS with minimized capacity and reduced cost, it will be advantageous to use them many times a day to allow for the time-shifting of demand and to supplement the grid during high demands. This new paradigm of energy use will be greatly effective when Time of Use (ToU) tariffs are applied in developed countries such as the UK. Whereas, for developing countries with intermitted power grids or remote areas with no access to a grid with the renewables and diesel generator (DGen) being the only means of power supply, the need for fast response storage capable of withstanding multiple cycles a day becomes more important.

This research presents the use and assessment of flywheel storage systems as an alternative to chemical batteries to supplement solar PV systems backed up by diesel generators. The introduction is followed by a description of FESS in Section 2 and its control and analysis in Section 3. Formation of the model of a standalone hybrid solar PV system including a detailed description of the residential demand model is provided in Section 4. The results of the analysis along with the impact of the flywheel system in reducing diesel generator fuel consumption are discussed in Section 5.

2. Description of Flywheel Energy Storage

A flywheel energy storage system (FESS) is a simple device that stores energy in rotational momentum and driven by a direct drive integrated motor-generator (MG) to operate as an electrical storage. The FESS is comprised of a spinning rotor, MG, power electronics, bearings, and safety containment, as shown in Figure 2. The rotary kinetic energy in a flywheel system is stored in its core element as a rotating mass given by the equation below.

$$E = \frac{1}{2} I \omega^2.　\text{(1)}$$

where E is the stored energy (Joules), I is the moment of inertia (kg·m^2), and ω is the angular speed (rad/s).

The electrical power in and out of the MG and power transfer to a load or the grid is controlled with a power electronics operated inverter similar to battery storage or any other non-synchronous device. For a reasonable size of the MG and in order to avoid excessively high voltage variations, the flywheel speed is kept between a maximum and a minimum (typically o-third to one-half its full

speed) and is kept spinning by a small input torque to account for the parasitic losses of the system. The usable energy of flywheel storage can be determined by Equation (2) shown below.

$$E_{usable} = \frac{1}{2} I \left(\omega_{\max}{}^2 - \omega_{\min}{}^2 \right) = \frac{1}{2} I \omega_{\max}{}^2 \left(1 - \frac{\omega_{\min}{}^2}{\omega_{\max}{}^2} \right) \tag{2}$$

Flywheel state of charge (SOC) is maintained by operating the rotor at the desired speed by overcoming the standby losses arising due to bearing friction and aerodynamic drag, where the latter can be virtually eliminated by use of a sealed casing to hold the vacuum level. The power flow in a flywheel system can be managed by the size of the MG and is independent of the rotor, which provides the possibility of producing higher power capacities with a fairly small FESS suitable for a few tens of seconds or minutes.
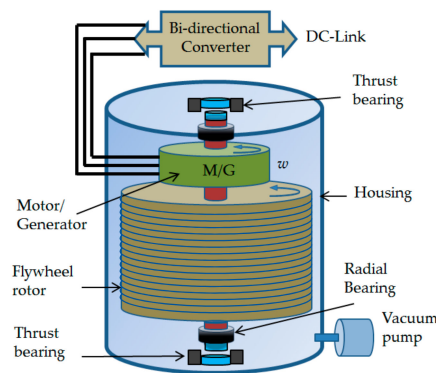

Figure 2. Structure and components of a flywheel system.

The technology of flywheels for energy storage has significantly advanced with the development of materials technology, bearings, and power electronics [11]. Flywheels with the main characteristics of high power and energy density and high efficiency compete with other storage systems in transportation, military services, space satellites, and in electrical energy storage applications [12,13]. With the storage capacity of up to hundreds of MJ and power ranges from kW to GW, flywheels can perform in a range of vital energy storage applications in an electrical power system [14]. On the downside, the main drawbacks associated with flywheels are their higher capital cost and self-discharge rate as well as safety issues, which is always recommended to be dealt with at the highest priority by investigating the rotor failure mechanisms and associated containment structure and material [15]. While the physical principle underlying FESS is simple, sometimes the devices themselves may be fairly complex with high-end measurement equipment, the type of the rotor (i.e., fiber composite), magnetic load compensation, and bearing assembly (i.e., HTS magnetic bearing).

A detailed description of the structure and components of flywheel storage is discussed in reference [16], and characteristics and comprehensive portrayal of its applications are studied in reference [17]. The use of FESS, as a low-cost alternative to chemical batteries, for decentralized PV systems is studied in reference [18]. Power quality improvement and UPS are the most common applications of flywheels in electrical energy storage [19,20]. The major contenders to flywheels for these applications are limited to electrochemical batteries and supercapacitors. However, the batteries are highly incompatible and they suffer from an insufficient life cycle due to the required higher number of cycles per day [21]. Particularly for power quality applications, electrical disturbances are short but quite frequent, with the vast majority of them diminishing in less than 5 s. Given the longer life cycle and fast response time of flywheels, they offer an improvement over batteries in managing such disturbances effectively. However, an electrochemical battery would require approximately 3650 cycles in 10 years with only one cycle per day, which is quite unlikely under these circumstances. This can be only achieved if the battery is carefully managed (both electrically and thermally) and the

depth-of-discharge (DoD) is kept low [10]. To reduce the DoD, the energy storage needs to be sized two to five times the required capacity, which leads to increased costs. Supercapacitors have been tested for these types of applications and their operational lifetime is relatively low (reaching at best 12 years) [2]. However, with more or less the same capital cost, flywheels will have an operational lifetime in excess of 20 years with almost an infinite cycle life [6]. Despite their longevity, due to the cost and safety issues as well as the level of complexity of flywheels in comparison to batteries, there are a limited number of real-world onsite installations of FESS and this is mainly dominated by the Beacon Power in the USA region [17]. Therefore, what has been proposed in this research is a flywheel system based on steel laminates in view of overcoming the cost and safety issues associated with, respectively, the fiber composite and solid steel flywheels.

## 3. Control and Analysis of Flywheel Energy Storage

The power conversion system involving different forms of storage systems can be presented as shown in Figure 3. It shows the connection of the flywheel storage to an electrical grid through a DC-link. However, the same configuration can be used when connecting other storage systems (batteries, supercapacitors, or SMES) to the grid. All storage types link to the same DC bus and they are connected to the grid at the point-of-common-coupling (PCC). The components that the storage systems commonly share are the switchgear, transformer, AC filter, and the grid side converter (GSC), which communicates with the storage side converter (SSC) to maintain the voltage at the DC link.
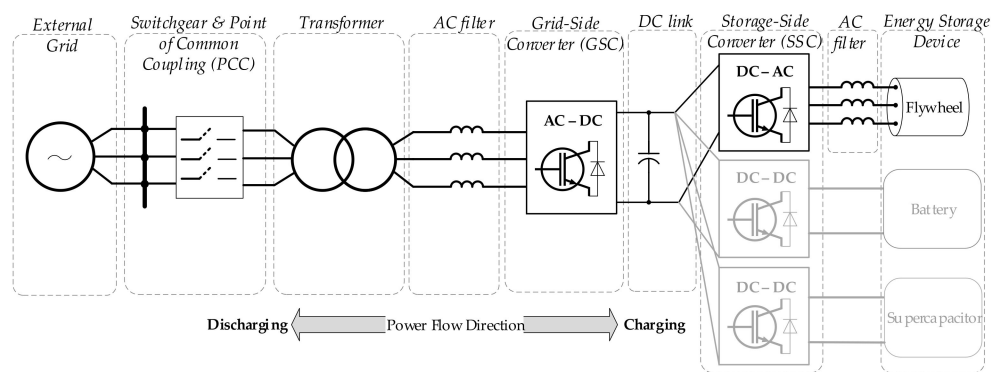
Figure 3. General configuration of the power conversion system involving different energy storage systems adapted from reference [22].

What generally differentiates between the operation of a flywheel storage system and other storage systems is the topology of the SSC. It functions as a bidirectional AC-DC inverter to control the supply of power in and out of the flywheel, whereas, in the case of other storage systems such as batteries, supercapacitors, and SMES, it performs as a bidirectional DC-DC converter to communicate between the DC-link and the storage device. For flywheels, the converters are arranged in a cascaded bidirectional back-to-back AC-DC-AC configuration to perform power flow in both directions with the help of an associated control system.

A generalized topology of the flywheel storage with a bi-directional power converter connected to an electrical grid is shown in Figure 4. The electrical supply and the FESS are connected through the DC-link and back-to-back converters. The power flow on the grid side is controlled by the GSC while the SSC controls the operation and flow of power in and out of the MG connected to the flywheel rotor. Therefore, the operation and energy conversion of the FESS is controlled by the MG.
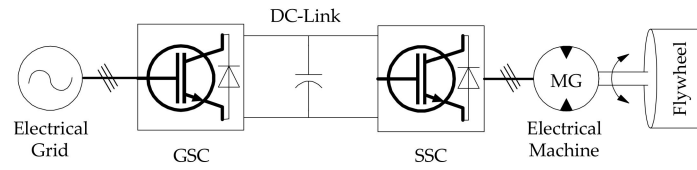
Figure 4. FESS with back-to-back bidirectional power converters.

3.1. Description and Mathematical Model of Permanent Magnet Synchronous Machine

The working principle of the FESS can be discussed in three modes of operation: charging mode, discharging mode, and standby mode. During charging, SSC draws power from the DC-link to run the MG and accelerate the flywheel. MG is operating as a motor, SSC as an inverter, and GSC as a rectifier to maintain the DC-link voltage. While discharging, the operation of both converters is reversed and the flywheel is decelerated to deliver energy and maintain the DC-link voltage. The standby mode is when the flywheel spins at a constant fixed speed and no energy conversion occurs except for a small power fed into the flywheel to maintain speed.

In this research study, a permanent magnet synchronous motor (PMSM) is considered to be an integrated electrical machine to perform the energy conversion in the FESS. It is commonly used in motion control applications due to its low inertia, compact structure, high specific power, higher efficiency, and high steady-state torque density [23]. Based on its attributes and due to its fast dynamic response, PMSM is usually considered for high-speed flywheel applications compared to induction machine (IM) and variable reluctant machine (VRM). Recently, it has been broadly used in variable speed applications thanks to its low losses, reduced size, and simple method of control [24–27]. Contrary to the other motors, a PMSM has no windings on the rotor and it operates based on the magnetic field produced by its own permanent magnets. The main drawbacks of PMSM are its high self-discharge rate due to the stator eddy current losses, its low tensile strength, and its high price [19].

The decoupled voltage balance equations of the PMSM in the *d–q* rotating reference frame are represented in Equations (3) to (8). The transformation of three-phase *a-b-c* voltage equations to their respective *d–q* equations helps control the machine and, therefore, allows separation of flux producing and torque producing components of the AC machine along the *d*-axis and *q*-axis, respectively [28].

$$V_q = R_s I_q + \omega_e \lambda_d + \frac{d\lambda_q}{dt} \tag{3}$$

$$V_d = R_s I_d - \omega_e \lambda_q + \frac{d\lambda_d}{dt} \tag{4}$$

where

$$\lambda_d = L_d I_d + \lambda_m \tag{5}$$

$$\lambda_q = L_d I_q \tag{6}$$

Substituting the above in Equations (3) and (4) and simplifying gives t following equations.

$$V_q = R_s I_q + L_q \frac{dI_q}{dt} + \omega_e L_d I_d + \omega_e \lambda_m \tag{7}$$

$$V_d = R_s I_d + L_d \frac{dI_d}{dt} + \omega_e L_q I_q \tag{8}$$

Similarly, the electromagnetic torque developed by the motor in terms of *d–q* components can be obtained using the equation below.

$$T_e = \frac{3}{2}\frac{P}{2}\left(\lambda_m I_q + \left(L_d - L_q\right)I_d I_q\right) \tag{9}$$

Considering a non-salient cylindrical rotor PMSM, the magnetic resistance is the same in all directions and equal inductances ($L_d = L_q$) can be assumed. The electromagnetic toque in Equation (9) can be simplified and will depend only on the rotor flux (λ_m) and stator current (I_q).

$$T_e = \frac{3}{2}\frac{P}{2}\lambda_m I_q \tag{10}$$

Lastly, the mechanical torque and electromagnetic torque relation is presented by the equation below.

$$T_e = J\frac{d\omega_m}{dt} + B\omega_m + T_L \tag{11}$$

where I_d and I_q are the direct and quadrature axis stator currents (A), L_d and L_q are the direct and quadrature axis inductances (H), J is the combined moment of inertia of the flywheel and PMSM (kg·m^2), B is the viscosity friction (N·m/rad/s), T_e is the electromagnetic torque (N·m), T_L is the load torque (N·m), ω_m is the rotor's mechanical speed (rad/s), and P is the number of poles.

3.2. Operation and Control of FESS and MG

The torque of AC motors is instantaneously controlled using the vector control technique where both the magnitude and direction of the motor currents are controlled. Field-oriented control (FOC) and direct torque control (DTC) are the main controlling techniques for instantaneous torque operations where the former is more popular and widely used despite its higher level of complexity [29]. The operation of FESS requires variable speed control and instantaneous torque changes are required for high performance and smooth operation for the entire speed range. In this study, the Field-oriented Vector Control using a space vector pulse width modulation (SVPWM) technique has been used to control the operation and dynamic performance of the PMSM operated flywheel (PMSM-Flywheel) during the acceleration and deceleration modes. A comprehensive description of SVPWM and PMSM control methods are addressed in References [29–33]. A generalized representation of the Vector Control transformation is shown in Figure 5.
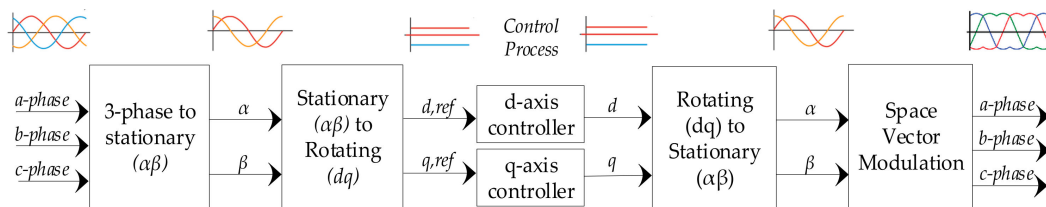

Figure 5. Vector control transformation adopted from reference [31].

The control block diagram of the PMSM-Flywheel for the charging (motoring) and discharging (generating) states is presented in Figure 6. The operation of the SSC is controlled by cascaded control loops with an inner current loop and an outer speed loop to regulate the speed of the PMSM-Flywheel. The controlling operation of the cascaded loops is performed using PI controllers. In the inner control loop, the Clark-Park transformation is used to transform the measured three-phase stator currents to two-axis *d*–*q* currents. The flux and torque of the MG are controlled separately by the decoupled *d*–*q* currents using PI current controllers. The *d*-component of the current is the flux producing component and the *q*-component is the torque producing component [33]. Similarly, in the outer loop, the PMSM-Flywheel speed is measured and regulated by comparing it with the reference speed. The torque of the machine is controlled by applying the output of the speed regulator as the reference *q*-current component for the current regulator.

During the discharge mode when the voltage of the DC-bus drops below a specified threshold value, a voltage controller is required to regulate the DC-link voltage by adjusting and controlling the currents. This action is controlled by the GSC, which functions to maintain a constant DC voltage and

regulate the reactive power of the grid [22]. The outer voltage-loop in the discharging mode, therefore, replaces the outer speed-loop in charging. In contrast to the motoring mode, in the generating mode, the measured DC-link voltage is regulated and provided as input for the current PI controller to produce the relevant gate signals to the GSC.

The FESS state-of-charge can be determined and monitored with the speed loop, which is also crucial for better utilization of flywheel's useful energy by controlling its operation between a minimum and maximum speed range. The status of the position and speed of the flywheel rotor in different states of operation is essential for controlling its flux and torque, in order for it to operate within a desired speed range. Similarly, if the PMSM-Flywheel speed is known, the DC bus voltage can be controlled by governing the MG torque and, hence, power.
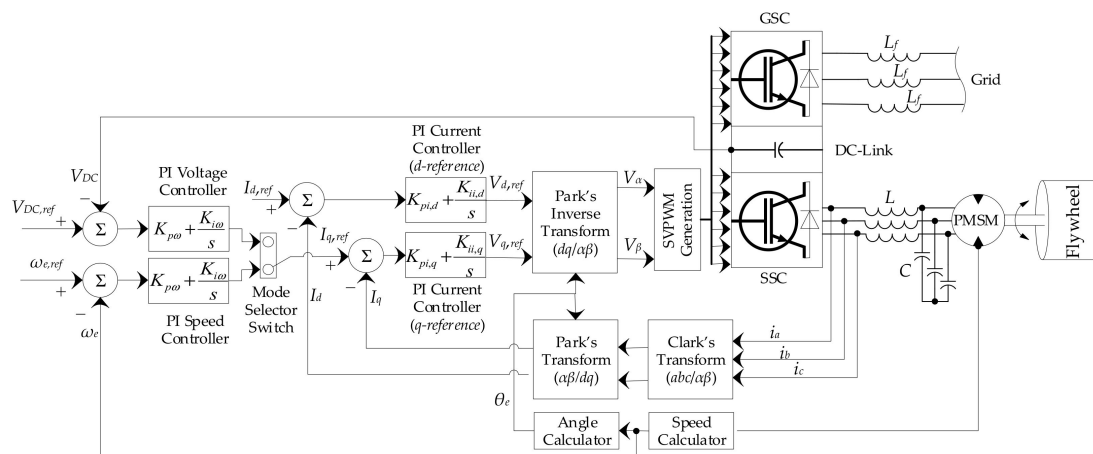

Figure 6. Block diagram of the FESS controlling scheme.

4. Model of the Standalone Hybrid Solar PV System

This study describes an interesting application where it proposes to reduce fuel burn and emissions in residential properties in which electrical power is provided by an islanded solar PV system with a backup diesel generator. Such systems are common in areas with weak or non-existent grids, particularly in developing countries, and this is where the demand for electrical power is increasing at the fastest rate. It is proposed that a flywheel would be good fit for this application given the attributes of long calendar life, fast response time, high charge-discharge rates, and low environmental impact, as opposed to an electrochemical battery, which would suffer from high cycle storage as required in this application. Flywheels are much less sensitive to temperature, which would be an added benefit given off-grid islanded systems are often installed in countries with higher temperature climates. It is here that the testing of this hypothesis is reported in terms of developing a control strategy, quantifying energy savings, and assessing how the flywheel will perform as compared with an Li-ion battery.

The model of a combined islanded PV system, diesel generator, and FESS supplying a dynamic variable load has been implemented in MATLAB/Simulink and the results are presented and analyzed in detail. All system components are connected to a common DC bus for better utilization of the energy and ease of control (Figure 7). The connected load has been chosen to be a typical residential load with variable demand throughout the day so that the operation and communication between the available sources of energy (PV, DGen, and FESS) are tested for close to real-life conditions. The load demand profiles were generated using CREST Demand Model that is a high-resolution energy demand model for building occupancies at the residential level [34].
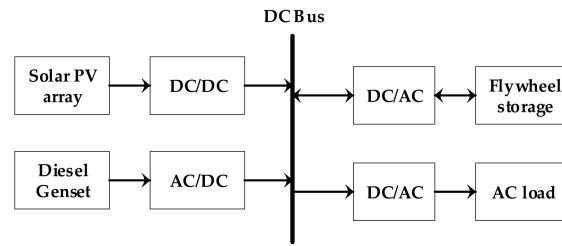
**Figure 7.** General configuration of a PV, DGen, and FESS connected to a load via the DC bus.

4.1. FESS Model

A simplified model of the flywheel storage system consisting of a permanent magnet MG connected to an electrical grid via a DC link is illustrated in Figure 8. The torque command governs the motoring or generating states of the MG based on which the charging and discharging states of the flywheel is determined. The standby state, however, is controlled with a zero-torque command and the operation of the system is governed by the aerodynamic drag and bearing friction, which are both embedded in the flywheel model to account for idling losses. The output generated signals indicate the electromagnetic torque and three-phase stator currents of the MG as well as the state of charge (SOC) and stored energy of the flywheel system.
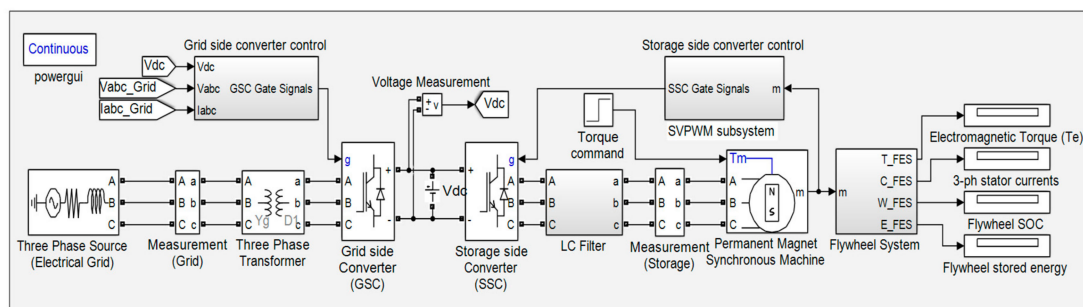
Figure 8. The simplified model of a PMSM operated flywheel connected to an electrical grid.

There are two feedback controlling schemes in place to provide the means of communication between the flywheel and the grid in order to maintain the voltage level at the DC-link. The power flow from the grid side is controlled by switching the gates of the IGBT/Diode operated converter. The DC-link voltage along with the three-phase voltages and currents from the power grid are regulated by comparing with respective reference values to generate the gating signals for the GSC. Similarly, the gating signals of the SSC are generated through a feedback loop from the terminals of the PMSM. However, the controlling scheme of the SSC is more complicated because it has to maintain the DC-link voltage and control the speed of the flywheel during its charge, discharge, and standby modes. This is implemented using the SVPWM described in Section 3.2 (Figure 9).
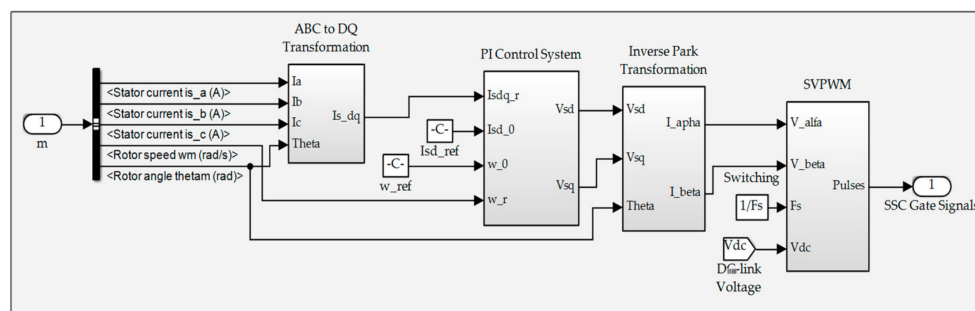

Figure 9. Space vector pulse width modulation (SVPWM) subsystem.

4.2. Model of Residential Load Demand

An excellent residential load demand has been developed from the CREST demand model that is a high-resolution stochastic model of integrated electrical-thermal demand at a domestic level [34]. The model calculates electrical demand based on appliances, lighting demand, and active resident occupancy. To account for load variations and random load spikes, the model uses a bottom-up approach to create "spikiness" from the simulation of switching the appliances *on* and *off*. Similarly, the natural behavior of occupants in using the appliances at home is determined. Although this is based on the UK time-use survey data [35], it is considered applicable to other countries with the exception of the air conditioning load, which could be added if needed following the same methodology as described in this paper. The data is used to generate stochastic profiles of the houses in order to consider different states such as the residents being active at home, asleep at home, or away from home and active, which is naturally related to use of appliances and, hence, the electrical demand [34]. The key parameters required for generating the load profiles are the day of the month, the month of the year, type of the day, the number of dwellings, and the total number of residents in a single dwelling unit. Figure 10 shows typical load profiles in February generated for two dwellings each with five residents. Typically, there are two peak times during the course of 24 h where the time of the peak is generally dependent on the type of the day—whether a weekend or a weekday. However, the peak times on a weekend is shifted and the occupants typically wake up late and sleep late (Figure 10). Additionally, the load distribution is quite irregular throughout the day and the occupants are active but perform different tasks at different times. The energy consumption on a weekend is also higher in comparison to a weekday given that the occupants are mainly at home.
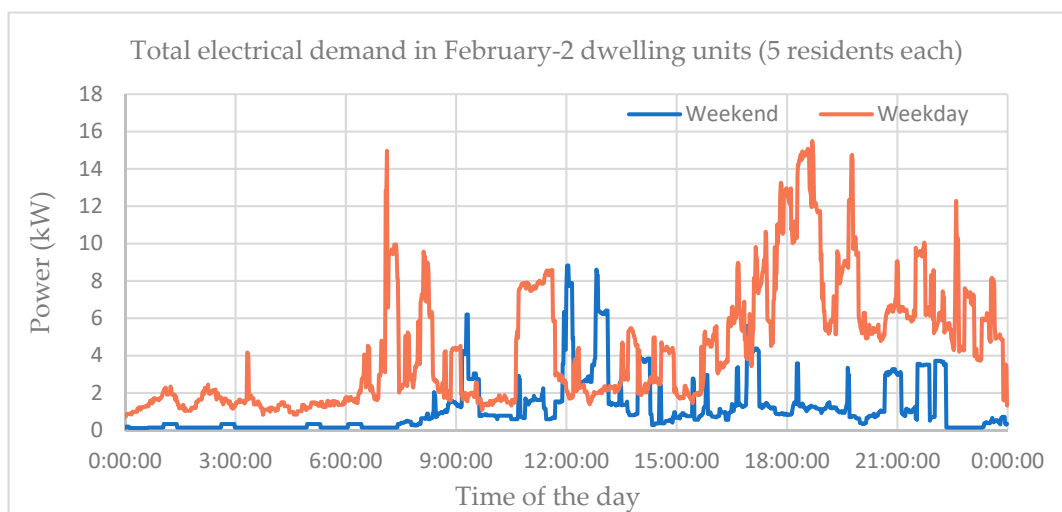

Figure 10. Total electricity demand for two dwelling units in February.

Considering the load pattern described earlier, three different load demand profiles were created to analyze the dynamic performance of the hybrid solar PV, DGen, and FESS. The load profiles are generated for weekends and at different times of the year to demonstrate total electrical demand for 10 dwellings with five residents each. The weekend is selected since the total demand for a weekend is usually higher when compared to a weekday and the load peaks and load spikes are inconsistent since they occur at different times of the day and do not follow any specific pattern. Hence, the designed system will be tested for close to real circumstances but under extreme conditions and for worst-case scenarios. For ease of analysis and a better comparison of the results, a duration of three hours is considered for each case. From each load profile, the peak times with the highest load demand and more frequent load variations are selected for analysis.

4.2.1. Load Profile 1

Profile 1 represents the total electrical demand for 10 dwellings on a January weekend (Figure 11). The morning peak demand starts to increase after 8 am and will diminish at 1 pm. The afternoon peak demand starts at 3 pm and lasts until 8:30 pm including a random spike at around 7 pm. The load demand for a duration of 3 h between 17:30–20:30 pm is selected for analysis (Figure 12). This includes a 15 kW peak demand during which the performance of the hybrid system will be very important.
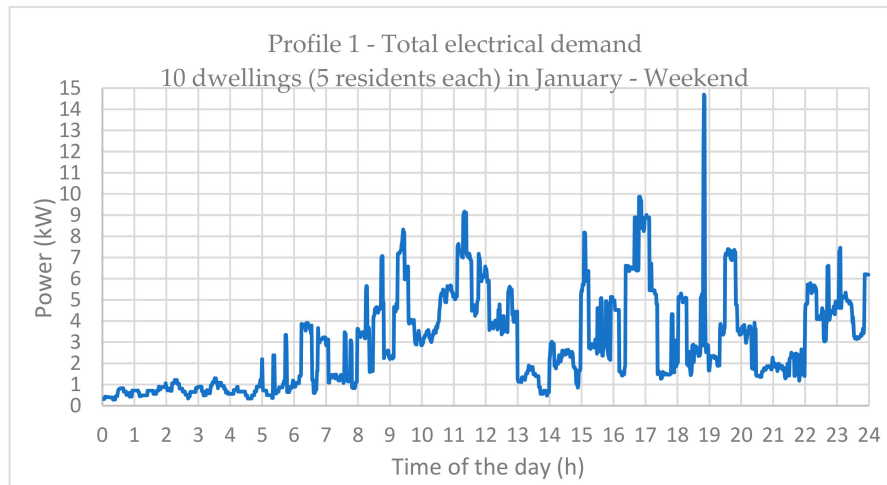
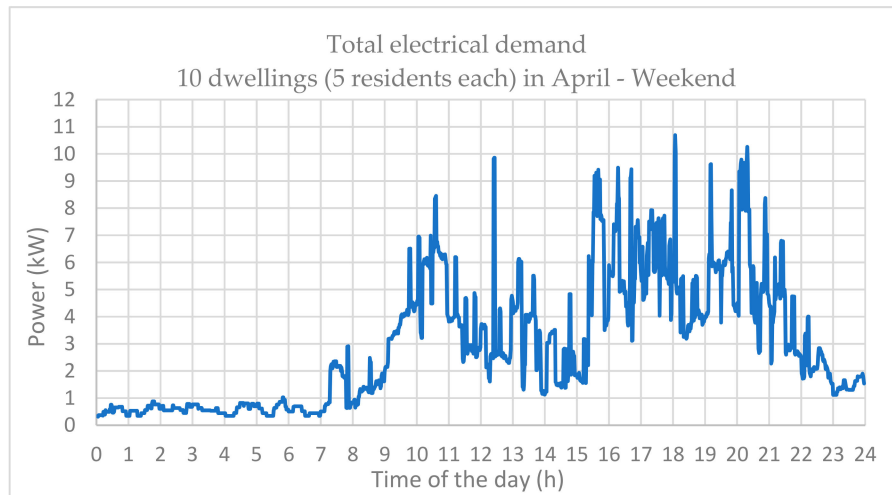**Figure 11.** 24-h total electrical demand—Profile 1.
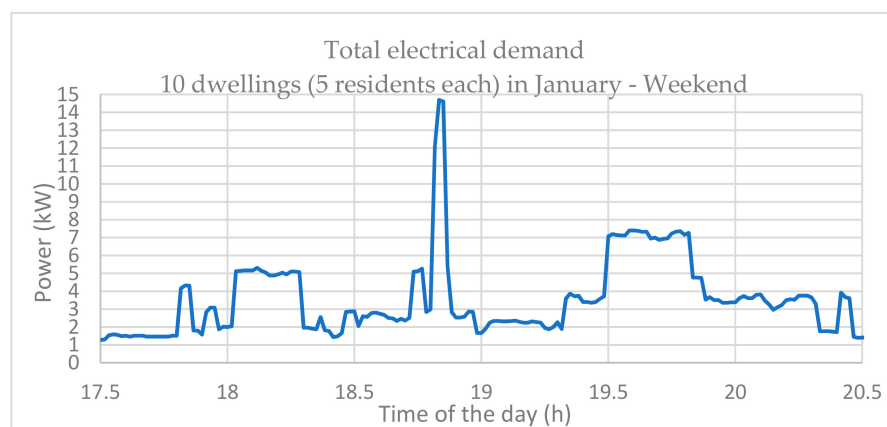
Figure 12. 3 h (17:30–20:30) total electrical demand—Profile 1.

From the perspective of the solar PV system or diesel generator, it will be a challenge to provide energy for this type of load (especially during the afternoon peak). The average demand for this load profile is about 5–6 kW but the PV system and the diesel engine must be designed for the maximum load of 15 kW even though it lasts for only a short period of only 5 min. This is when integration of a storage system becomes important and FESS best suits such conditions providing bulk power in a short duration.
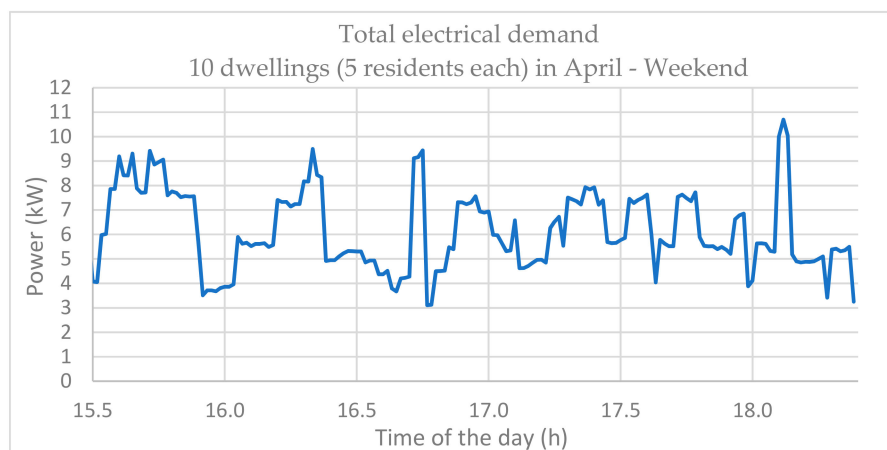
4.2.2. Load Profile 2

Profile 2 represents the total electrical demand for 10 dwellings on an April weekend (Figure 13). This profile is relatively different to profile 1 because the peak times last longer and are quite scattered throughout the day. The morning peak lasts between 9 am and 3 pm while the afternoon peak starts at around 3 pm and lasts until 10 pm. The average load demand is also higher in the afternoon peak and, therefore, the 3-h peak time between 3:30–6:30 p.m. is selected for analysis (Figure 14). During this

time, the load profile comprises the most fluctuations and the highest peak demand also falls within this period. Hence, the energy source, whether it is going to be a PV system, a DGen, an FESS, or a combination of these, will be hardly resting.
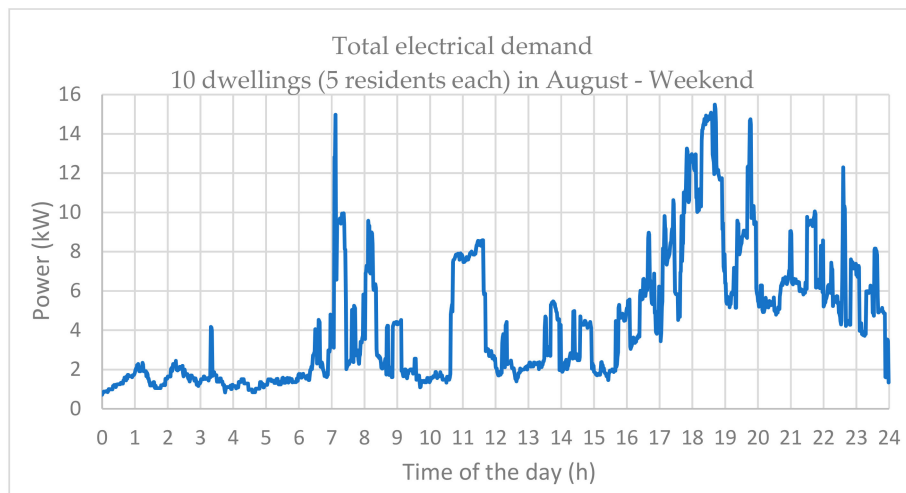

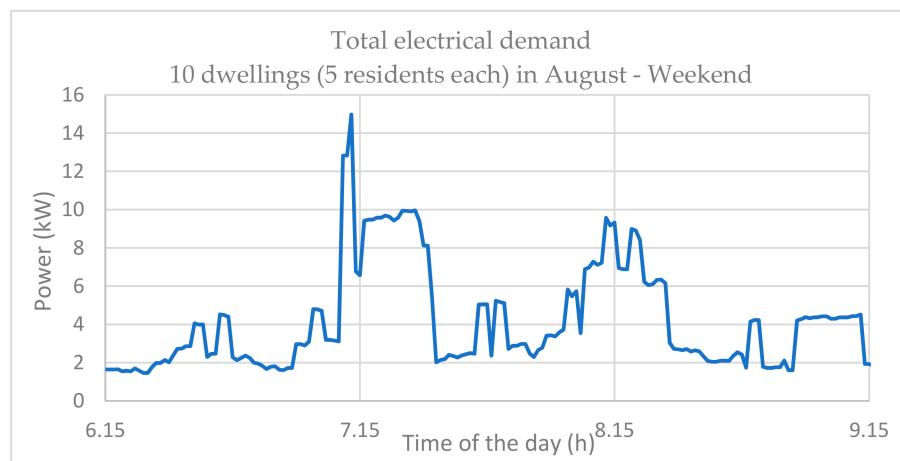**Figure 13.** 24-h total electrical demand—Profile 2.

Figure 14. 3 h (15:30–18:30) total electrical demand—Profile 2.

4.2.3. Load Profile 3

Figure 15 shows a load profile 3 representing the total electrical demand for 10 dwellings on a weekend in August. Apart from load profiles 1 and 2, the load demand is distributed in three peaks with a different time distribution and pattern. The morning peak starts early and lasts approximately 2 h with two sharp spikes reaching a maximum of up to 15 kW. The demand starts to increase again after 10:30 a.m. and descends back at 12 p.m. The afternoon peak demand lasts longer (4 p.m.–12 a.m.) with numerous load fluctuations, which is quite similar to the afternoon peak demand for load profile 2. Hence, the designed system will be tested for a similar situation under load profile 2, but with higher peak demands with longer durations. Therefore, the morning peak demand between 6 a.m.–9 a.m. is considered for analysis (Figure 16).

**Figure 15.** 24-h total electrical demand—Profile 3.

Figure 16. 3 h (06:15–09:15) total electrical demand—Profile 3.

Considering the generated load profiles and referring to Figure 7 where the load is connected to a common DC bus between the DGen, PV system, and FESS, it will be interesting to test the operation and dynamic performance of the system in supplying energy to these load demands.

4.3. Hybrid FESS-PV-DGen Model

The model of the diesel generator was developed using the built-in Simulink blocks available in the MathWorks computing environment [36]. The synchronous diesel engine is connected to an IGBT/Diode operated AC-DC converter to maintain the voltage level at the DC bus when the engine is generating power. The operation of the generator side converter is controlled using a similar control scheme applied for controlling the switching mechanism of the GSC connected to the FESS. The asynchronous diesel engine was chosen rather than a variable speed generator since it is most likely that this type of lower cost device would be already available and the solar PV and FESS would be added to an existing system to reduce cost rather than have to replace the entire system.

The diesel engine model can be connected to an AC or a DC load. However, it is integrated to the PV system and flywheel at the DC-link, which serves as the point of common coupling between the energy sources and the load (Figure 7). The fuel consumption of the diesel engine relative to load is shown in Figure 17 and its parameters are provided in Table 1. The rate of fuel consumption at lower power ratings (i.e., close to 25% loading) is larger than the consumption at 100% load due to the fixed losses having a greater effect as power decreases.
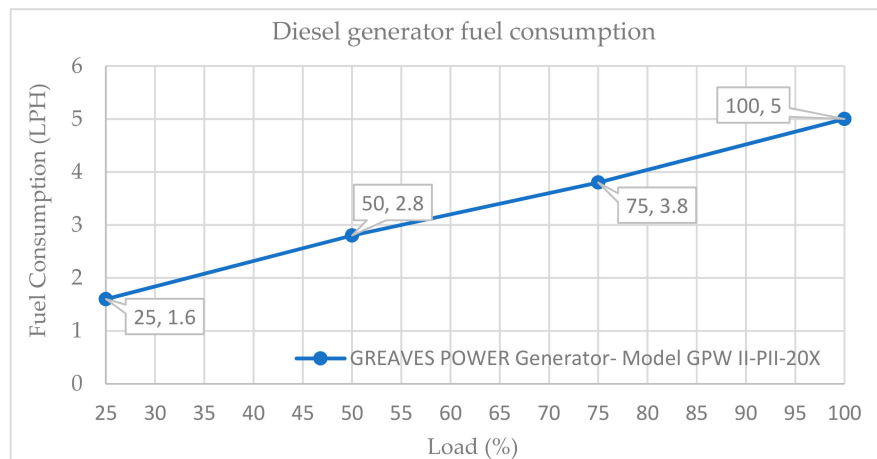
Figure 17. Diesel engine fuel consumption relative to the load.

Table 1. Parameters of the hybrid FESS-PV-DGen model.

Energy Source	Parameter	Value (Unit)
PMSM-FESS	Stator resistance	0.20 (Ω)
	Armature inductance ($L_d = L_q$)	0.0438 (H)
	Combined inertia (steel laminate rotor and MG)	11 (kg·m^2)
	Number of poles	2 (poles)
	Power rating	10 (kW)
	Energy storage rating	5 (kWh)
	Self-discharge rate	230 W/Cycle
	Operational losses	310 Wh/Cycle
	Input voltage	380 (V)
	Rated frequency	417 (Hz)
	Inverter switching frequency	10 (kHz)
	Filter damping resistance	0.75 (Ω)
	Filter capacitance	40 (μF)
	Filter inductance	0.64 (mH)
	GREAVES POWER Generator GPW-ll-Pll-20X	
Diesel Generator (Synchronous Machine)	Nominal power	15 (kW)
	Line-to-line voltage	380 (V)
	Rated frequency	50 (Hz)
	Number of poles	4 (poles)
	Sun Power SPR-315E-WHT-D NREL System Advisor Model	
Solar PV array (2 parallel strings x10 series-connected modules per string)	Maximum power	315 (W)
	Open circuit voltage	65 (V)
	Voltage at maximum power point	54.7 (V)
	Current at maximum power point	5.76 (A)
	Sun irradiance	500 (W/m^2)
	Cell temperature	40 (deg. C)
	DC-link voltage	600 (V)

The PV module is adapted from the existing PV array examples available in MathWorks [37] with the solar radiation data complying with the residential demand model in reference [34]. The model of a solar PV array system is connected to the DC-bus through a boosted DC-DC converter (Figure 7). The MATLAB/Simulink built-in PV array block requires the sun irradiance (W/m^2) and cell temperature (deg. C) as inputs and produces PV voltage and current as outputs. The parameters of the PV module can be user-defined or selected from a wide range of pre-set modules from the NREL System Advisor Model. Further details on the mathematical model and internal circuit of the PV module including a variety of control techniques are addressed in References [38,39].

The hybrid model of PV-DGen-FESS is developed based on the controlling schemes and standalone models of the flywheel, PV system, and diesel generator described earlier. The main difference, in this case, is that the model of the flywheel previously connected to an electrical grid (Figure 8) will now be connected to the solar PV system serving as the main source of energy supply. The set of parameters for each subsystem is provided in Table 1. The connected load is a dynamic three-phase load updated on a timely basis from a lookup table that stores the energy consumption data of residential households described in Section 4.2.

5. Results, Analysis, and Discussions

In this study, the impact of the integration of flywheel storage into the combined diesel generator and solar PV system is investigated. The purpose is to off-load the diesel generator as much as possible to improve system efficiency and reduce fuel consumption and CO_2 emissions. It is proposed that the introduction of the flywheel will improve overall system reliability by taking the load off the generator as well as filling the gaps between the supply and demand due to any system instabilities.

The total electrical demand is shared between the PV system, the flywheel, and the diesel engine while assuming fully sunny days where the PV array can constantly provide power to supply an average demand load. Additionally, the flywheel storage and the diesel engine cover anything above the average. The PV system has been sized for 6 kW maximum based on the average demand for all load profiles, and this is kept the same for all scenarios for a fair comparison. The diesel generator has to be sized for the maximum load demand to account for the cases when neither of the PV or FESS is available.

The load above the average rating is initially covered by FESS and the diesel generator will be turned off for fuel savings. For example, if the load is greater than 6 kW, the FESS will take over from the PV system and start discharging to supply the demand. In occasions where the load is less than 6 kW and the flywheel is fully charged, the flywheel will switch to a standby mode. The generator will come on only when the power source from both the PV system and FESS is not available. For instance, the flywheel is already discharged and the PV system cannot provide power due to a cloud pass or when the load demand is above its maximum rating. It will turn off as soon as the power is available from either of the PV or FESS sources. Considering this, the storage device will come on and off multiple times during the day, which will suit flywheel applications.

The flywheel is a C2 rating type with 10 kW PMSM integrated MG capable of storing 5 kWh when operating between 10,000–20,000 rpm. Therefore, it can provide power to the load when it is between 6 kW–15 kW. Figure 18 shows a power transfer flow chart of the hybrid FESS, PV, and DGen system.
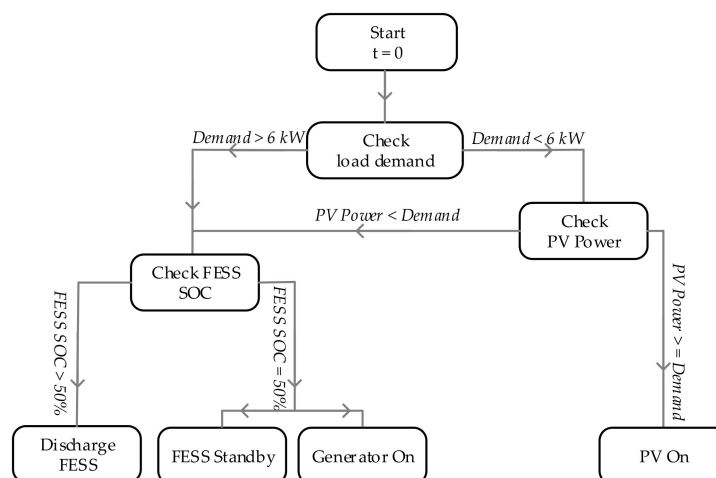

Figure 18. Power transfer flow chart of FESS, PV, and DGen.

The flywheel's charge-discharge is controlled based on the communication of the PV system with the load. It is discharged when the demand is above a 6 kW rating of the PV system and supplies power to the load until its minimum state of charge (50% SOC) is reached and the flywheel is switched to a standby mode. The 50% SOC criterion is used to allow an equal amount of energy to be stored or released in the case that it is not clear, which will be required. At the times of excess PV supply due to lower demand, the surplus available power is utilized to charge the flywheel. The FESS acts as an intermediate energy source due to its fast response characteristic. The simulated results of the hybrid systems dynamic performance during the energy transfer for each load profile are discussed in the following subsections.

5.1. Load Profile 1

The load profile 1 and power output of the solar PV system along with the state of charge of the flywheel system is shown in Figure 19. Throughout the course of 3 h, the demand is mostly lower than the maximum rating of the PV system except for the two peaks arising at t = 80 min and t = 120 min. With the flywheel initially at its minimum 50% SOC, there is surplus energy available to charge it up to more than 95% before it discharges at t = 80 min to cover the peak demand (Figure 19c). After brushing the short load spike, it starts to charge again until it reaches 100% SOC and switches to a standby mode for approximately 18 min (t = 102–120 min).
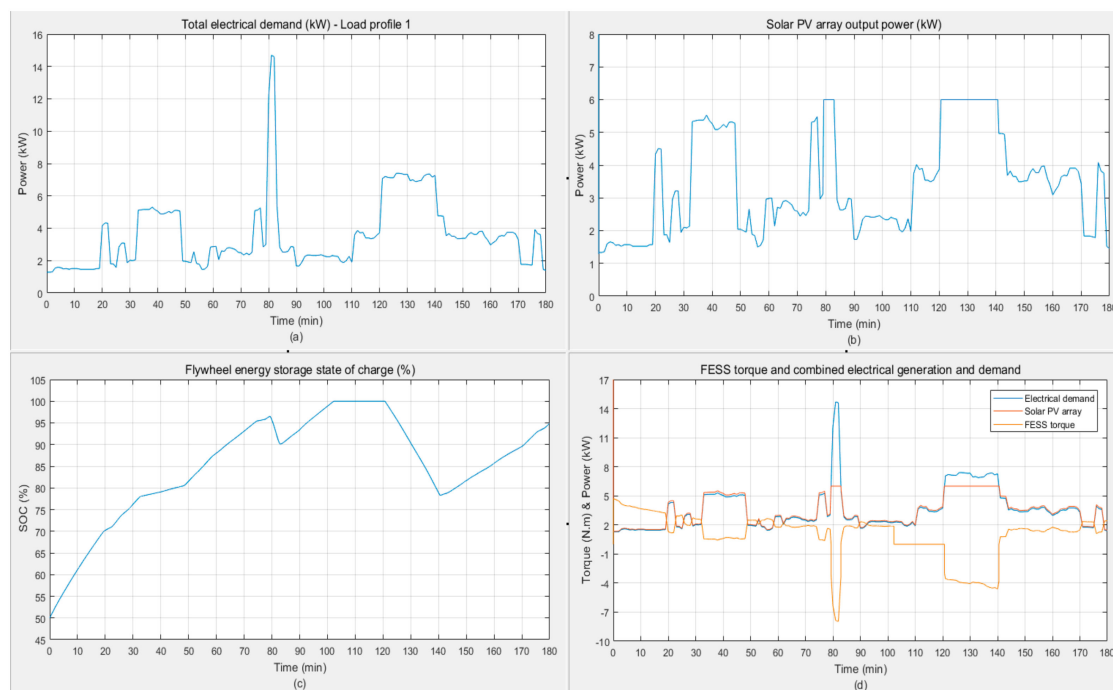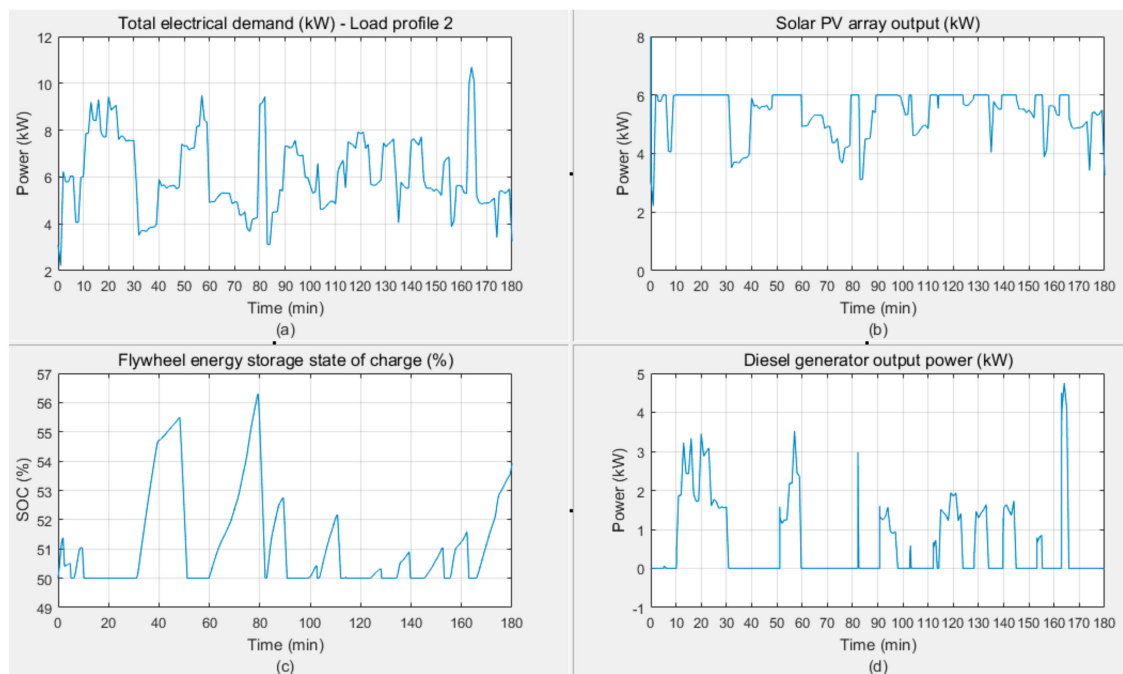

Figure 19. (**a**) Load profile 1. (**b**) PV array output power. (**c**) Flywheel state of charge. (**d**) Flywheel torque, combined generation, and demand.

The combined plots in Figure 19d indicate how the FESS utilizes the available excess energy of the PV system during charging. When the demand is low, more power is available and, therefore, the positive (charging) torque is higher. The same can be concluded about the negative (discharging) torque, which occurs during the peak demand times where the flywheel discharges to supply the surplus in demand (t = 120–140 min). The zero-torque condition shows the flywheel standby status (t = 102–120 min). Comparing the scenarios for the cases with and without storage, it can be seen that the integration of the flywheel fully rested the diesel generator and it was not called even during the times of peak demand.
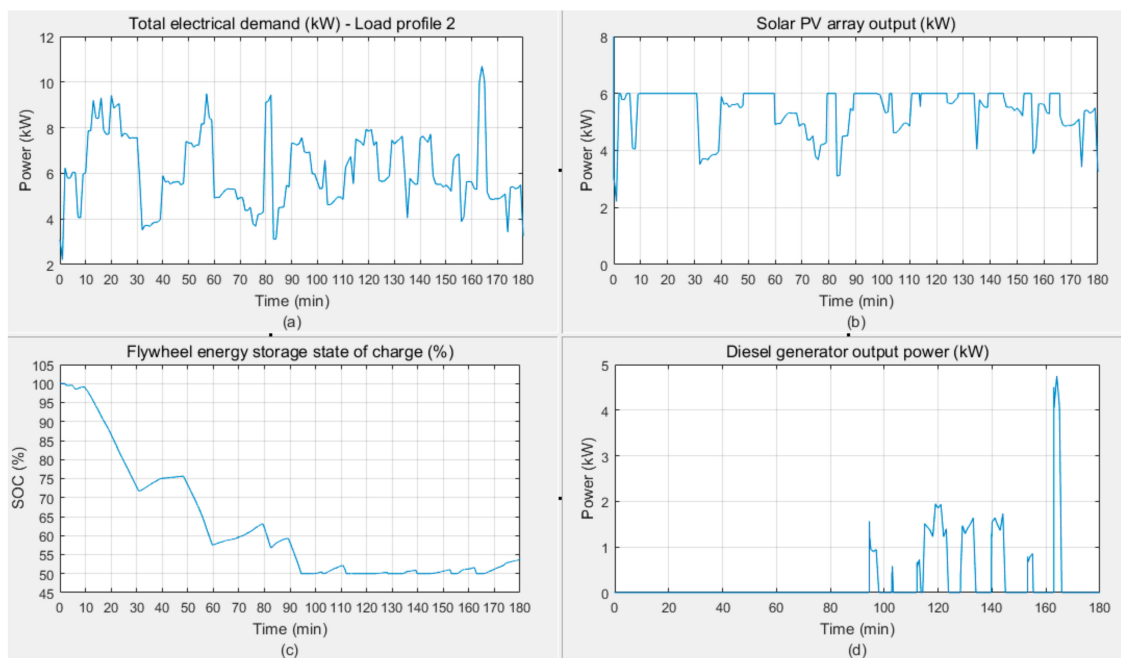
5.2. Load Profile 2

Compared to load profile 1, the conditions for load profile 2 is very challenging since the demand varies for the whole 3-h period with many lengthy peaks. This implies that the backup energy sources (DGen or FESS) will be in service continuously (Figure 20). The first peak demand appears at t = 10 min when the load is above 6 kW and the flywheel is needed to cover the surplus in demand. However, since the flywheel is at its minimum charge level (50% SOC), it switches to standby mode and the generator is called to supply the load (Figure 20c,d). Shortly after (at about t = 30 min) when the load demand decreases, the flywheel starts charging using the surplus power available from the PV system. This charging and discharging process of the flywheel continues until the end but the charge state is not improved due to the nature of the demand. It partially helps the diesel generator with the peak demands, but, despite this, the generator is still active and running frequently—catching up with the supply shortage from the PV system (Figure 20d). It can be seen that the generator is turned on when the FESS is in a standby mode. Otherwise, the flywheel will be either charging or discharging.


Figure 20. (**a**) Load profile 2. (**b**) PV array output power. (**c**) Flywheel initially at 50% state of charge. (**d**) Diesel generator output power.

The above situation can be improved if the flywheel is initially fully charged (100% SOC) and can deliver energy immediately when demanded. Since the major peak demands appear at the beginning of load profile 2, a fully charged flywheel can keep the generator off for a longer period, as shown in Figure 21. The flywheel discharges at t = 10 min and covers the excess demand for about 85 min before it reaches 50% SOC and switches to a standby mode. The power output plot of the diesel generator shows how the flywheel has reduced the operation time of the generator (Figure 21d).

The initial charging condition of the flywheel is vital in reducing the load on the generator. Therefore, the system is examined for 50%, 75%, and 100% SOC scenarios and the results are shown in Figures 22 and 23. The voltage and currents of the diesel generator and PV system for the case of a fully charged flywheel is presented in Figure 24 showing the compliance of the model. There is a large current spike (t = 164 min) due to a sudden increase in the load and commanding an instant diesel generator engagement. The DC-link voltage drop is also slightly more than 5 V at this instant. However, it is still not too far from the acceptable ±5% voltage drop level.

Figure 21. (**a**) Load profile 2. (**b**) PV array output power. (**c**) Flywheel initially at 100% state of charge. (**d**) Diesel generator output power.
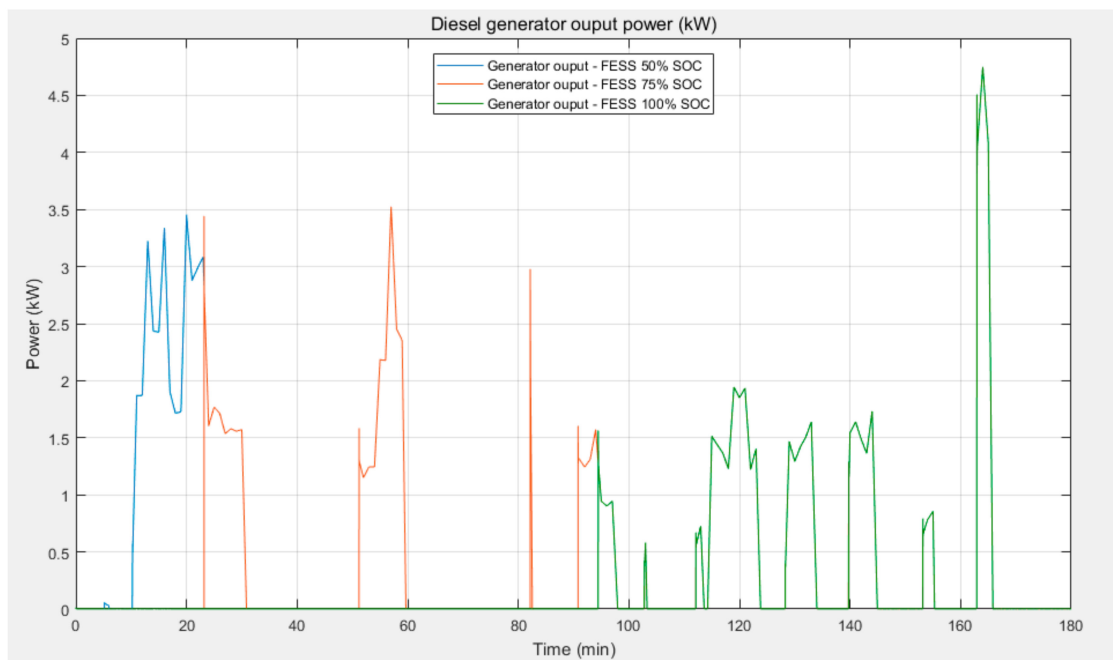
Figure 22. Generator output power based on the initial state of charge of the flywheel system.
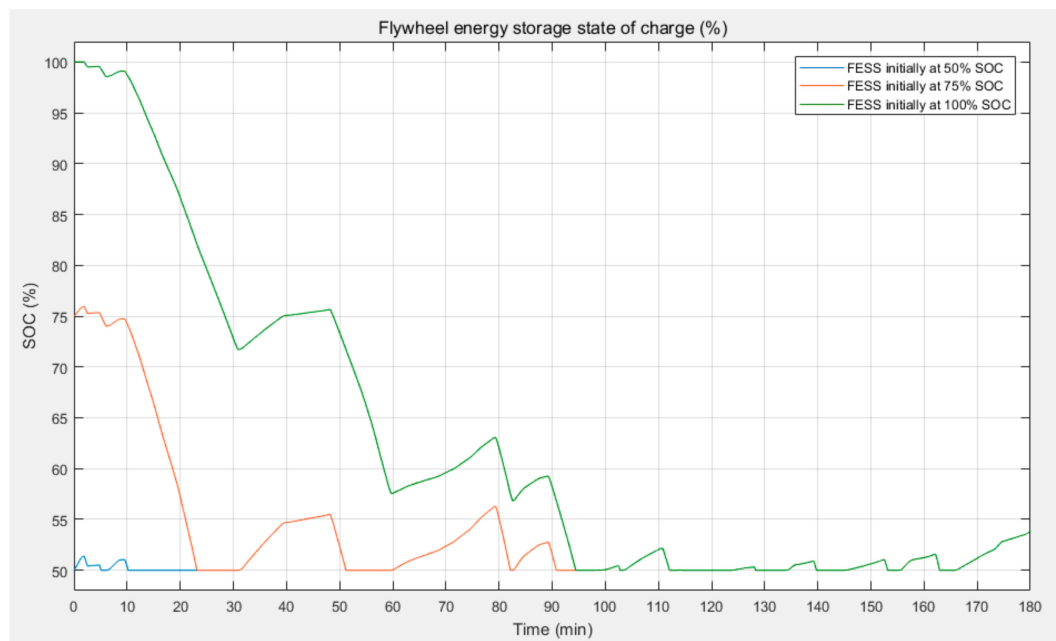
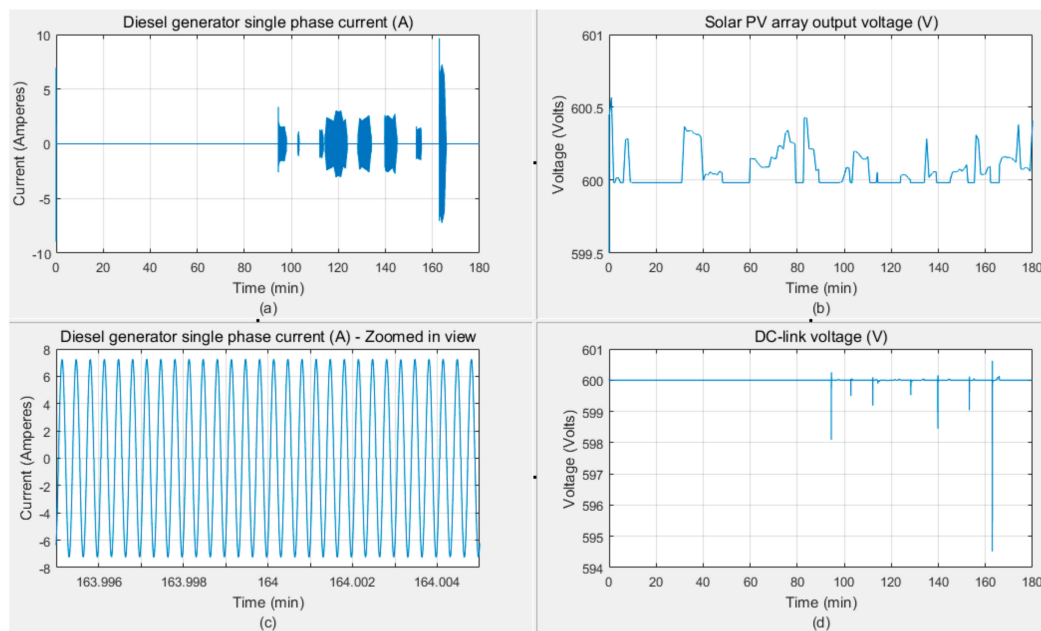**Figure 23.** Flywheel charge-discharge plots at different states of charge.

Figure 24. System parameters. (**a**) Diesel generator single-phase current. (**b**) PV array output voltage. (**c**) Diesel generator single-phase current- zoomed-in view. (**d**) DC-link voltage.

5.3. Load Profile 3

The operation of the hybrid system in supplying power to load profile 3 is shown in Figure 25. There are two main peak demands that would require power contribution from the FESS in addition to the PV system. However, the main difference to the previous scenarios is that the higher demand appears later and the surplus power from the PV system allows the flywheel to charge before it is called for action (at about t = 55 min). Due to the higher peak demand, the flywheel discharges faster and reaches its minimum charge level before switching to a standby mode (Figure 25c). Hence, although lasting for a short period, there are only two occasions where the flywheel runs out of power and the generator is turned on to take the surplus demand (Figure 25c).
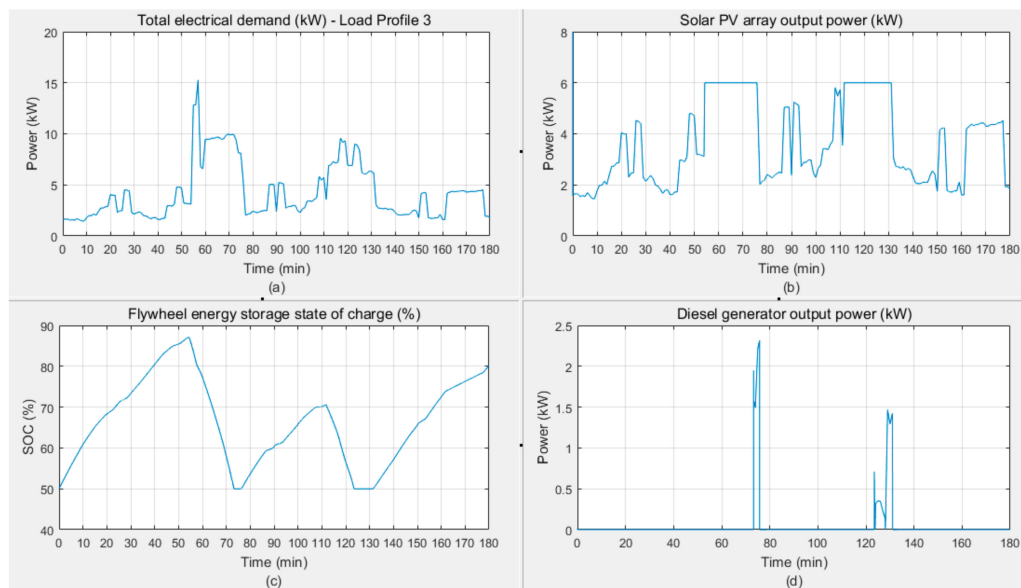
Figure 25. (**a**) Load profile 3. (**b**) PV array output power. (**c**) Flywheel initially at 50% state of charge. (**d**) Diesel generator output power.

The system performance and communication between the PV system, the FESS, and the backup DGen are shown in Figure 26. Notice how the flywheel utilizes the surplus energy from the PV system to charge. The generator currents comply with the generator power output plots. The DC bus voltage is maintained constant for the whole duration by the PV and FESS except when the diesel generator comes on and introduces small voltage fluctuations (Figure 26d).
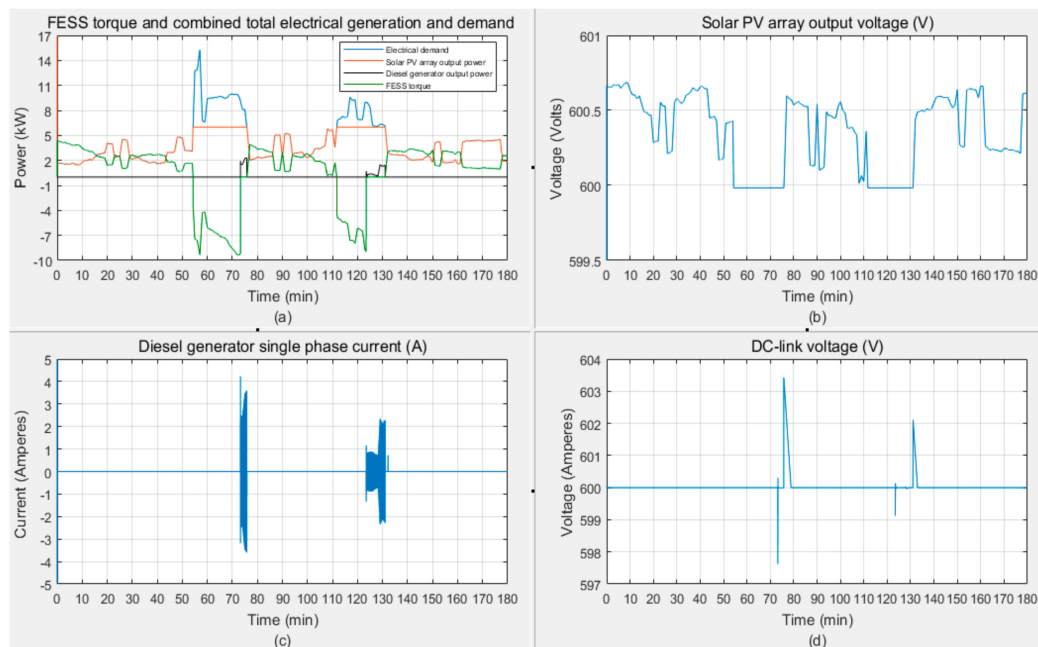
Figure 26. (**a**) Combined operation of the FESS, DGen, and PV system. (**b**) PV array output power. (**c**) Diesel generator current. (**d**) DC-link voltage.

In the above scenario, if the flywheel was initially at a 75% charged state, the generator would not be needed at all and the peak demands can be fully covered by the FESS. This is because the flywheel reaches 100% SOC before the first peak demand appears and it will have enough energy stored to

brush up the peak. Under these multiple charge-discharge conditions, the flywheel standby time is very short and the self-discharge rate will be very small and negligible.

5.4. Analysis of FESS Impact on Generator Fuel Consumption

The operation of the diesel generator in each of the above scenarios has been dependent on the contribution of the flywheel storage system. There have been instances that the demand has been fully supplied by the combined operation of the PV system and flywheel while the generator was turned off for the whole period. On the contrary, the higher demand on some occasions (i.e., profile 2) mostly required full engagement of the FESS as well as the backup diesel engine. Therefore, an analysis of the FESS contribution in reducing generator fuel consumption is discussed in this section. Generator fuel consumption and fuel cost savings for all different load profiles are calculated including the cases when the diesel engine is in partial or full operation. The diesel generator model is selected from standard datasheets provided by the generator manufacturers. The tabulated results show the generator's produced energy (kWh) along with the fuel consumption (liters) and maximum fuel cost savings (£) for different load profiles.

The diesel generator consumption and fuel savings in relation to FESS's impact are summarized in Tables 2–4. The results of the analysis show that the flywheel's involvement and contribution in reducing diesel consumption were dependent on its initial state of charge. In addition, the system was also analyzed for the conditions of without storage assuming that the FESS was not available and the surplus demand was entirely covered by the diesel engine. The results of this analysis are shown in Table 4 and a summary of the main findings showing the flywheel impact on cost and generator output reduction is presented in Figure 27.

Table 2. Diesel generator fuel consumption.

Load Profiles and FESS SOC	Ratio of Consumption at Percentage Load [2]		Energy Generated	Fuel Consumed		Max Fuel Cost in 3 Hours [1]
	(l/kWh)		(kWh)	(l)		(£)
	75%	100%		75%	100%	
Profile 1	0.25	0.33	0	0	0	0
Profile 2 (Flywheel 50% charged)	0.25	0.33	1.962	0.5	0.65	0.84
Profile 2 (Flywheel 75% charged)	0.25	0.33	1.567	0.4	0.52	0.67
Profile 2 (Flywheel 100% charged)	0.25	0.33	1.144	0.3	0.38	0.5
Profile 3 (Flywheel 50% charged)	0.25	0.33	0.7124	0.2	0.24	0.31

[1] Cost of fuel = 1.3 (£/l) [2] GREAVES POWER Generator G20-II.

Table 3. Diesel generator fuel consumption—stand alone and without FESS.

Load Profile	Ratio of Consumption at the Percentage Load [2]		Energy Generated	Fuel Consumed		Max Fuel Cost in 3 Hours [1]
	(l/kWh)		(kWh)	(l)		(£)
	75%	100%		75%	100%	
Profile 1	0.25	0.33	8.651	2.163	2.855	3.71
Profile 2	0.25	0.33	14.35	3.59	4.74	6.16
Profile 3	0.25	0.33	10.14	2.54	3.35	4.35

[1] Cost of fuel = 1.3 (£/l) [2] GREAVES POWER Generator G20-II.

Table 4. FESS impact on reducing generator fuel consumption and fuel cost.

FESS Contribution		Load Profiles				
		Profile 1	Profile 2			Profile 3
Flywheel Initial State of Charge (%)		**50**	**50**	**75**	**100**	**50**
DGen output (kWh)	Without Flywheel	1.067	2.3	2.3	2.3	1.95
	With Flywheel	0	1.96	1.57	1.14	0.71
DGen energy reduction (%)		100	15	32	50	64
DGen fuel cost saving in 3-h (£)		0.46	0.15	0.31	0.5	0.53
DGen fuel cost saving per day (£)		3.68	1.2	2.48	4	4.24
DGen fuel cost saving per year (£)		1350	440	905	1460	1550
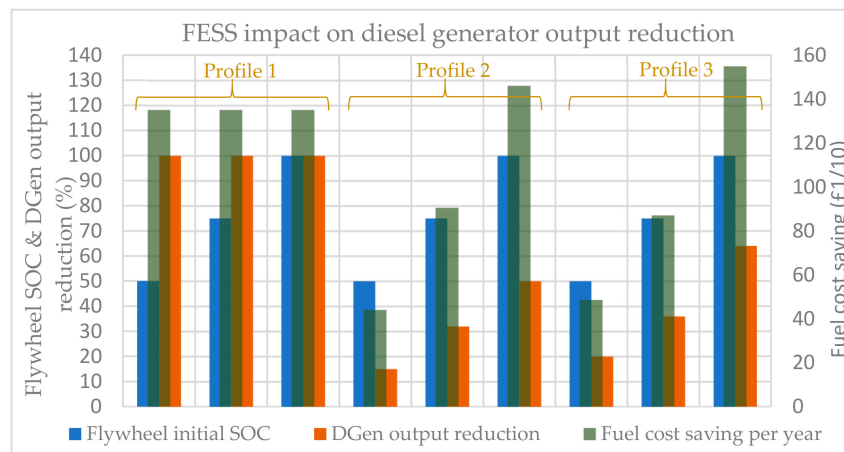
Figure 27. Diesel engine output reduction and cost savings relative to flywheel SOC.

On some occasions, the flywheel storage fully rested the diesel generator (i.e., load profile 1) when the PV, DGen, and FESS were operating as a hybrid system. For load profile 2 that both the flywheel and diesel generator were quite engaged due to the nature of the demand, the FESS can contribute up to 50% of the DGen load and bring approximately £1460 savings per year. In the worst-case scenario when the initial stored energy of the flywheel was at a minimum (50% SOC), it has contributed toward reducing the operation of the diesel engine by 15% with nearly £440 savings per year. Furthermore, in the case of load profile 3, the flywheel impact in terms of percentage reduction in diesel generator supply has been approximately 65% with a total annual fuel savings of £1550 per annum.

Comparing the scenarios for the cases of with and without the storage, it was shown that integration of the flywheel helped reduce the load on the diesel generator and, in some conditions (i.e., load profile 2), the diesel engine was fully rested including the times of peak demand. Introduction of a FESS as a backup storage system not only provides fuel reductions and fuel savings but also increases diesel generators' efficiency and lifetime. It adds stability to the system that would, otherwise, not be achieved with a standalone PV system backed up by the diesel generator. In addition, from the environmental perspective, reducing the service of the diesel engine will reduce greenhouse gases due to CO_2 emissions. Analysis of the flywheel impact on reducing CO_2 emissions shows a minimum of 0.915 MT CO_2-eq savings due to the reduction of the diesel generator load. Nevertheless, for the cases of load profile 1 and 3 where the flywheel had a greater impact, the level of CO_2 reduction was approximately 2.8 and 3.2 MT CO_2-eq, respectively.

6. Conclusions

The research work presented described the assessment of small-scale energy storage flywheel systems for use in residential premises with highly intermittent or non-existent grid infrastructure. This was carried out to assess the hypothesis that FESS would be a suitable alternative to a Li-ion

battery for an islanded electric system comprising of a diesel generator and solar PV. This question was addressed by modelling and analysis of an FESS-integrated into a standalone solar PV system with a backup diesel engine supplying residential loads based on a number of different energy transfer strategies. The operation of the hybrid system was analyzed for close to real-life situations and, for each case, the communication and responsiveness of the model in terms of supplying the total electrical demand and the outputs of the PV system and the diesel generator as well as the flywheel storage was analyzed and the results were presented. The analytical results for the electrical characteristics of the system, such as currents and voltages of the generator and the flywheel system, output voltage of the PV system, and the DC-link voltage, were also presented. Since the use of flywheels has been very limited in residential applications due to their higher cost and safety requirements, this research considered a flywheel system based on steel laminates to overcome the cost and safety issues associated with, respectively, the fiber composite and solid steel flywheels.

The analysis of generator fuel consumption showed that the availability of the flywheel storage had great impact on the diesel engine fuel consumption. The findings of this research showed that, in some conditions, the flywheel contribution had led to about 65% reduction in operation time of the diesel generator. The impact of the FESS was dependent on its initial state of charge and complexity of the demand. The calculated minimum annual fuel cost savings imposed by the flywheel system for the cases of combined PV-DGen-FESS was about £440 per annum. On the other hand, in scenarios where the stored energy of the flywheel was fully utilized to supply the demand and the diesel engine was very rarely used, a maximum annual fuel cost saving of £1550 per year was achieved.

On the number of cycles, the results of the analysis show that the flywheel system was operating with at least two cycles during the course of 3 h. In some instances, the number of cycles was increased to three or four depending on the type of load and initial SOC of the flywheel. If the same ratio were assumed for a full day, then the number of charge-discharge cycles for the flywheel system would reach at least 10 cycles per day, 3650 cycles per year, and 73,000 cycles over 20 years. Considering this, the storage device will come on and off multiple times during the day, which will suit flywheel applications. In contrast, if a chemical battery (i.e., Li-Ion type) was used to arrange for backup storage services under such circumstances, it will be experiencing multiple charge-discharge cycles per day with some cycles not even fully completed. For a Li-ion battery to perform 73,000 cycles, the cells would need to be replaced approximately 12 times over the 20 years for a C1, 10 kWh battery operating with a 50% depth of discharge, based on life estimates from reference [10]. This assumes the battery was kept within a small temperature range and with a good battery management system.

Lastly, it was concluded that the use of a flywheel storage system was not only limited to generator fuel reduction and savings but could also increase the diesel engine's average efficiency and lifetime. It adds stability to the system that would, otherwise, not be achieved with a standalone PV system without storage and only backed up by the diesel generator. In addition, from the environmental perspective, reducing the service of the diesel generator will reduce greenhouse gases due to CO_2 emissions. The findings of this research show that the integration of the flywheel system as a backup storage could reduce the emission level by up to 3.2 MT CO_2-eq in a year. Had a chemical battery storage been used, it would suffer from too much degradation given a large number of discharge cycles needed, so it is believed flywheels offer a good alternative to batteries for this application.

The research for future work will focus on a detailed cost analysis based on levelized cost of storage (LCOS) of flywheel and battery storage for use in hybrid solar PV systems in islanded operation. Another area of research that the authors would like to explore in the future is a mathematical optimization approach to optimize the control algorithm of the flywheel storage system when integrated into a hybrid solar PV system.

Conflicts of Interest: The authors declare no conflict of interest.

References

1. Chen, H.; Cong, T.N.; Yang, W.; Tan, C.; Li, Y.; Ding, Y. Progress in electrical energy storage system: A critical review. *Prog. Nat. Sci.* **2009**, *19*, 291–312. [CrossRef]
2. Hadjipaschalis, I.; Poullikkas, A.; Efthimiou, V. Overview of current and future energy storage technologies for electric power applications. *Renew. Sustain. Energy Rev.* **2009**, *13*, 1513–1522. [CrossRef]
3. Del Granado, P.C.; Wallace, S.W.; Pang, Z. The Value of Electricity Storage in Domestic Homes: A Smart Grid Perspective. *Energy Syst.* **2014**, *5*, 211–232. [CrossRef]
4. European Commission, Directorate-General for Energy. DG ENER Working Paper; The Future Role and Challenges of Energy Storage. Available online: https://ec.europa.eu/energy/sites/ener/files/energy_storage.pdf (accessed on 29 August 2019).
5. Fu, Q.; Hamidi, A.; Nasiri, A.; Bhavaraju, V.; Krstic, S.; Theisen, P. The Role of Energy Storage in a Microgrid Concept: Examining the Opportunities and Promise of Microgrids. Available online: https://ieeexplore.ieee.org/document/6749070 (accessed on 29 August 2019).
6. Medina, P.; Bizuayehu, A.W.; Catalao, J.; Rodrigues, E.; Contreas, J. Electrical Energy Storage Systems: Technologies' State-of-the-Art, Techno-Economic Benefits and Applications Analysis. In Proceedings of the 47th IEEE Hawaii International Conference on System Science, Waikoloa, HI, USA, 6–9 January 2014.
7. Pullen, K.R. The Role of Flywheel Energy Storage in Decarbonised Electrical Power Systems. Energy Learning: United Nations UNEP-European Energy Centre EEC. Available online: https://energy-learning.com/index.php/opinion/78-what-s-new/162-flywheel-energy-storage (accessed on 9 November 2018).
8. Munoz, A.S.; Garcia, M.; Gerlich, M. *Overview of Storage Technologies*; Project SENSIBLE: A project funded by the European Unions Horizon 2020 research and innovation programme; European Union: Brussels, Belgium, 2016.
9. Dehghani-Saniji, A.R.; Tharumalingam, E.; Dusseault, E.; Fraser, R. Study of Energy Storage Systems and Environmental Challenges of Batteries. *Renew. Sustain. Energy Rev.* **2019**, *104*, 192–208. [CrossRef]
10. Schmidt, I.; Melchior, S.; Hawkes, A.; Staffell, L. Projecting the Future Levelized Cost of Electricity Storage Technologies. *Joule* **2019**, *3*, 81–100. [CrossRef]
11. Parfomak, P.W. *Energy Storage for Power Grids and Electric Transportation: A Technology Assessment*; Congressional Research Service-CRS Report for Congress; Congressional Research Service: Washington, DC, USA, 2012.
12. Hebner, R.; Walls, A. Flywheel Batteries Come Around Again: Kinetic energy storage will propel applications ranging from railroad trains to space stations. *IEEE Spectr.* **2002**, *39*, 46–51. [CrossRef]
13. Burchroithner, A.; Wegleiter, H.; Schweighofer, B. Flywheel Energy Storage Systems Compared to Competing Technologies for Grid Load Mitigation in EV Fast-Charging Applications. In Proceedings of the IEEE 27th International Symposium on Industrial Electronics (ISIE), Cairns, QLD, Australia, 13–15 June 2018.
14. Bolund, A.; Bernhoff, H.; Leijon, M. Flywheel energy and power storage systems. *Renew. Sustain. Energy Rev.* **2007**, *11*, 235–258. [CrossRef]
15. Buchroithner, A.; Haidl, P.; Birgel, C.; Zarl, T.; Wegleiter, H. Design and Experimental Evaluation of a Low-Cost Test Rig for Flywheel Energy Storage Burst Containment Investigation. *Appl. Sci.* **2018**, *8*, 22. [CrossRef]
16. Amiryar, M.E.; Pullen, K.R. Development of a High-Fidelity Model for an Electrically Driven Energy Storage Flywheel Suitable for Small Scale Residential Applications. *J. Appl. Sci.* **2018**, *8*, 453. [CrossRef]
17. Amiryar, M.E.; Pullen, K.R. A review of Flywheel Energy Storage System Technologies and Their Applications. *Appl. Sci.* **2017**, *7*, 286. [CrossRef]
18. Buchroithner, A.; Haan, A.; Preßmair, R.; Bader, M.; Schweighofer, B.; Wegleiter, H. Decentralized low-cost flywheel energy storage for photovoltaic systems. In Proceedings of the 2016 International Conference on Sustainable Energy Engineering and Application (ICSEEA), Jakarta, Indonesia, 3–5 October 2017.
19. Sebastian, R.; Alzola, R.P. Flywheel energy storage systems: Review and simulation for an isolated wind power system. *Renew. Sustain. Energy Rev.* **2012**, *16*, 6803–6813. [CrossRef]
20. Emadi, A.; Nasiri, A.; Bekiarov, S.B. Uninterruptible Power Supplies and Active Filters. In *Power Electronics and Applications Series*; CRC Press: Washington, DC, USA, 2005; pp. 19–24.

21. Bender, D. *Flywheels*; Technical report, SAND2015-3976; Sandia National Laboratories: Albuquerque, NM, USA; Livermore, CA, USA, 2015 May.

22. Diaz-Gonzalez, F.; Sumper, A.; Gomis-Bellmunt, O. Energy Storage Technologies. In *Energy Storage in Power Systems*; John Wiley & Sons Ltd.: West Sussex, UK, 2016; pp. 94–141.

23. Venna, S.G.; Vattikonda, S.; Mandarapu, S. Mathematical Modeling and Simulation of Permanent Magnet Synchronous Motor. *Int. J. Adv. Res. Electr. Electron. Instrum. Eng.* **2013**, *2*, 3720–3726.

24. Zhao, K. The study of Improved PI Method for PMSM Vector Control System Based on SVPWM. In Proceedings of the 2011 IEEE Industry Applications Society Annual Meeting, Orlando, FL, USA, 9–13 October 2011.

25. Zhang, Z.; Shu, J. MATLAB-based Permanent Magnet Synchronous Motor Vector Control Simulation. In Proceedings of the 2010 3rd International Conference on Computer Science and Information Technology, Chengdu, China, 9–11 July 2010; pp. 539–542.

26. Liu, T.; Tan, Y.; Wu, G.; Wang, S. Simulation of PMSM Vector Control System Based on Matlab/Simulink. In Proceedings of the 2009 International Conference on Measuring Technology and Mechatronics Automation, Zhangjiajie, China, 11–12 April 2009; pp. 343–346.

27. Soliman, H.M.; Hakim, S.M.L. Simple Model and PI Controller to Improve the Performance Characteristics of PMSM under Field Oriented Control with Using SVPWM. *Int. J. Adv. Eng. Nano Technol.* **2015**, *2*, 5–13.

28. Arroyo, E.L.C. Modelling and Simulation of Permanent Magnet Synchronous Motor Drive System. Master's Thesis, University of Puerto Rico, San Juan, PR, USA, 2006.

29. Kim, S.-H. Chapter 5: Vector Control of Alternating Current Motors. In *Electric Motor Control DC, AC, and BLDC Motors*; Elsevier: Oxford, UK, 2017; pp. 203–246.

30. Doe, H.V.; Shekokar, P.R.U. A Review of Speed Control Techniques Using PMSM. *Int. J. Innov. Res. Technol.* **2014**, *1*, 247–253.

31. Balazovic, P.; Filka, R. Sensorless PMSM Control for H-axis Washing Machine Drive. In Proceedings of the IEEE Annual Power Electronics Specialists Conference, Rhodes, Greece, 15–19 June 2008.

32. Jose, L.A.; Karthikeyan, K. A Comparative Study of Sinusoidal PWM and Space Vector PWM of a Vector Controlled BLDC Motor. *Int. J. Adv. Res. Electr. Electron. Instrum. Eng.* **2013**, *2*, 2662–2668.

33. Burgos, R.P.; Kshirsagar, P.; Lidozzi, A.; Wang, F.; Boroyevich, D.; Frame, A.A.D. Mathematical Model and Control Design for Sensorless Vector Control of Permanent Magnet Synchronous Machines. In Proceedings of the 2006 IEEE COMPEL Workshop, Rensselaer Polytechnic Institute, Troy, NY, USA, 16–19 July 2006; pp. 16–19.

34. McKenna, E.; Thomson, M. High-resolution Stochastic Integrated Thermal–electrical Domestic Demand Model. *Appl. Energy* **2016**, *165*, 445–461. [CrossRef]

35. Gershuny, J.; Sulivan, O. United Kingdom Time Use Survey, 2014–2015. UK Data Service. Available online: https://beta.ukdataservice.ac.uk/datacatalogue/studies/study?id=8128 (accessed on 8 December 2018).

36. MATLAB for Deep Learning. MathWorks. Available online: https://uk.mathworks.com/ (accessed on 3 November 2018).

37. PV Array Block MathWorks. Available online: https://uk.mathworks.com/search/site_search.html?suggestion=&c%5B%5D=entire_site&q=PV+array (accessed on 10 October 2018).

38. Viswambarau, V.K.; Ghani, A.; Zhou, E. Modelling and Simulation of Maximum Power Point Tracking Algorithm & Review of MPPT Techniques for PV Applications. In Proceedings of the 5th International Conference on Electronic Devices, Systems and Applications (ICEDSA), Ras Al Khaimah, UAE, 6–8 December 2016.

39. Gupta, A.K.; Saxena, R. Review on Widely-used MPPT Techniques for PV Applications. In Proceedings of the 1st International Conference on Innovation and Challenges in Cyber Security, Noida, India, 3–5 February 2016.